eEarth

Inflation of the Aira Caldera (Japan) detected over Kokubu urban area using SAR interferometry ERS data

D. Remy[1,2,*]**, S. Bonvalot**[1,2]**, M. Murakami**[3]**, P. Briole**[2]**, and S. Okuyama**[4]

[1]Institut de Recherche pour le Développement (IRD), UR154, France
[2]Institut de Physique du Globe de Paris, 4 Place Jussieu, 75005 Paris, France
[3]Geographical Survey Institute, Mizusawa Geodetic Observatory, Japan
[4]Kyoto University, Dept. of Geophysics, Kyoto, 606-8502, Japan
[*]presently at: Dept. of Geophysics, University of Chile, Santiago, Chile

Abstract. Nine ERS-1 and ERS-2 descending orbit data acquired over Aira Caldera between June 1995 and November 1998 were used to create 36 differential interferograms. Although the interferograms exhibit a relatively low level of coherence, even for couples sampling short time intervals (6 months), Synthetique Aperture Radar (SAR) observations reveal a distinct range change pattern over Kokubu urban area whose amplitude increases with the time separation between SAR images. The analysis of the ground deformation time series relative to the earliest ERS images showed a maximum uplift of about 20 mm between the north and the south of the urban area during the period covered by our satellite observations. Taking the reduced surface of the coherent area into account, we performed a simple modeling of the deformation field assuming an inflating spherical source within an elastic half-space medium located beneath the centre of the Aira Caldera. This simple model predicts a maximum volume increase of 20–$30 \times 10^6 \, \mathrm{m}^3$ between 1995 and 1998, which would produce an inflation of about 70 mm at the centre of the Aira Caldera and 40 mm in the Kokubu south urban area. These results are in good agreement with other geophysical observations carried out on the Aira caldera during this period. Despite the limited spatial extent of the coherent areas around the Aira Caldera, this study shows that DinSAR method using data collected in C band can be successfully used to detect subtle ground displacement changes of the volcanic complex and thus provides complementary information to ground-based geodetic monitoring of dynamic processes of the Aira Caldera and Sakurajima volcano.

Correspondence to: D. Remy
(remy@dgf.uchile.cl)

1 Introduction

Numerous papers have shown the potential of SAR (Synthetic Aperture Radar) interferometry data for ground deformation studies on volcanoes (Massonnet and Sigmundsson, 2000; Zebker et al., 2000; Pritchard and Simons, 2002). Under optimal conditions a differential interferogram derived from two SAR images may monitor topographic changes induced by internal volcanic processes with an accuracy of a few cm over periods of time up to several months or years. Furthermore, as satellite systems repeat their orbit on the order of weeks, it is now possible to generate deformation time series which help to better resolve time dependant deformation (Schmidt and Burgmann, 2003). In this paper we use the DinSAR method to examine ground deformation occurring on the volcanic complex of the Aira Caldera (Japan) within the 1995–1998 period (Fig. 1). This Caldera and its post-caldera volcano, Sakurajima, are among the most active volcanic centers in Japan where significant ground deformations have been observed from ground monitoring networks over several decades (Omori, 1916; Yokoyama, 1971; Aramaki, 1984). The latest precise leveling survey conducted along a coast road at Sakurijima clearly shows that the deflation of the ground around the Aira Caldera starting in 1974 turned into inflation in 1994 (Ishihara, 1999). Using JERS (L band, $\lambda=23.53$ cm) data acquired between 1993 and 1998, (Okuyama et al., 2001) detected two distinct deformation patterns. Figure 2 shows three examples of JERS interferograms used in their study for various time periods during 1993–1998. The first deformation pattern is located at the north flank of Sakurajima and it was interpreted by the authors as related to a volume change of a shallow
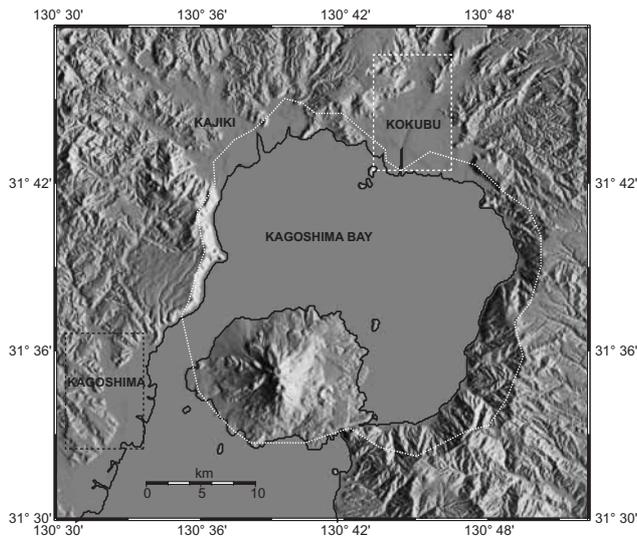
Fig. 1. Geographical setting of Kagoshima bay. The white dotted line is the rim of the Aira Caldera proposed by Matumoto (1943). The white box located in the northeast (Kokubu urban area) of the caldera shows the area used in this study for SAR data analysis and modeling. The black box located in the southwest of the caldera shows the area used to perform the analysis of the spatial structure of interferogram noise.

pressure source located beneath the volcano at 4 km depth. The second one corresponds to an uplift of Kokubu urban area, which was interpreted by the authors as related to a volume change caused by magmatic injection of a deep pressure source roughly located at the center of the Aira Caldera at 10 km depth. Assuming a point center of dilatation (Mogi, 1958), these authors estimated a roughly constant inflation rate of about 8–16×10^6 m^3/year between 1992–1998. In October 98 began an increase in seismic activity until July 1999 which has been interpreted as a migration of the magma stored in the magma reservoir beneath the caldera to the summit of Sakurajima volcano, accumulating stress in the rocks around the magma reservoir. This increase in seismic activity was followed by the eruptive activity which reached its peak between August 1999 and February 2000 (Smithsonian_Institution, 1999a, b, 2000; Kriswati and Iguchi, 2003).

Kriswati and Iguchi (2003) analyzed GPS data acquired from the Sakurajima Volcano Research Center network (12 permanent stations) and from 7 campaigns of Kyoto University in South Kyushu during 1996–2002 period in order to investigate characteristics of ground deformation caused by volcanic activity of Sakurajima. This study revealed an outward radial pattern of horizontal displacement from the center of the Aira Caldera. Assuming a simple point source of pressure in an elastic half space, the location of the source was estimated to be 8–9 km beneath the Aira Caldera. Between 1995 and 2000 the total volume change of the source was estimated to about 20×10^6 m^3. During the same pe-

riod total weight of volcanic ash ejected from the summit crater was estimated by the Sakurajima Volcano Research Center to about 8.75×10^9 kg which leads to an estimation of magma in volume to 3.5×10^6 m^3 (assuming a magma density of 2500 kg/m^3). Presumably, this preeruption uplift was caused by accumulation of magma within a reservoir beneath the Aira caldera prior to the 1999 eruption.

In this paper, we show a clear evidence of ground deformation of the northern rim of the Aira Caldera using ERS SAR interferometry, which is in good agreement with the previous independent studies. The analysis and interpretation of the interferogram time series are also presented

2 DinSAR data acquisition and processing

We analyzed a series of 36 interferograms produced from 9 ERS-1 and ERS-2 scenes acquired in descending orbits over the Aira Caldera volcanic complex between June 1995 and November 1998 (see Fig. 3). The differential interferograms were produced by the two pass method with DIAPASON software (CNES, 1996) using precise ERS orbit data produced by the Delft Institute for Earth-Oriented Space Research (DEOS)(Sharroo et al., 1998). The topographic contribution was removed by subtracting the fringe pattern computed from a Digital Elevation Model (DEM) with 45 m pixel spacing and with a height uncertainty of 5–10 m provided by the Geographical Survey Institute (Japan). The resulting interferograms span between 1 and 1261 days, with perpendicular baselines ranging from 2 m to 730 m (see Fig. 3).

Figure 4 shows typical examples of wrapped interferograms constructed using three different master images (orbits 20503, 23509 and 0386). It can be noted that the interferograms exhibit a relatively low level of coherence over the whole area due to densely vegetated areas and water surface which disconnects the Sakurajima volcano from the coast. The comparison between Fig. 2 and 4 clearly shows that the interferometric coherence is better and persists longer in L band than in the C band, confirming conclusions from InSAR investigations at others places (e.g., Murakami et al, 1996; Lu et al., 2005). Consequently using C band, successful measurements of the phase are only possible in three isolated areas located in the northeast (Kokubu urban area) in the northwest (Kajiki urban area) and in the southwest of the caldera (Kagoshima urban area). The two isolated areas corresponding to Kajiki urban area and Kagoshima urban area exhibit signals which are not observed in independent interferograms (i.e. generated from images pairs acquired from different satellite tracks). We conclude that these signals are mainly produced by atmospheric turbulence. On the contrary, examination of the differential SAR interferograms computed over time separations from one to three years reveals that Kokubu urban area exhibits a time dependant but perpendicular baseline independent phase pattern. This phase pattern (up to almost one fringe) cannot
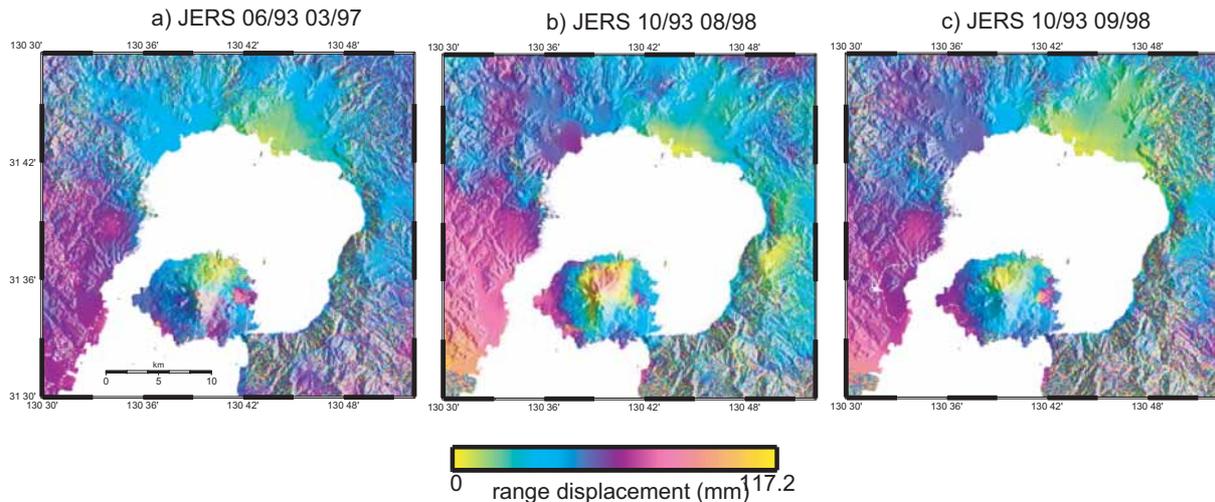
Fig. 2. Recorded differential JERS interferograms over the Aira Caldera encompassing the 1993–1998 period. **(a)** Interferogram spanning four years from June 1993 to March 1997. **(b)** Interferogram spanning five years from October 1993 to August 1998. **(c)** Interferogram spanning five years from October 1993 to September 1998. A complete cycle of phase (purple, blue yellow) represents a decrease in range of 11.73 cm between the ground surface and the satellite.

be attributed to topographic residuals resulting from DEM inaccuracies used in the data reduction as it does not appear in various interferograms obtained from images spanning over less than one month with orbit perpendicular baselines greater than 350 m. Effects of excess path delays produced by temporal changes of tropospheric water vapor content might also explain the interferometric signals on the Aira Caldera as they have been already observed on the study area (Remy et al., 2003). The signal seen here on Kokubu urban area is unlikely to be produced by topography related tropospheric effects as height variation along this coherent area is very weak (less than 200 m) and does not reveal any correlation with the observed phase signal. Obviously, we cannot rule out a possible contribution of residual transient tropospheric effects. According to the unpredictable character of atmospheric phase delay and without external data on the atmospheric water vapor content (such as direct or indirect measurements provided by radio-soundings, permanent GPS arrays, or MODIS/MERIS water vapor data, for instance), it is difficult to separate this phase delay from a signal of deformation. We discuss later (section analysis of the DinSAR time series) the influence of atmospheric effects on the interpretation of the observed signal in terms of displacement.

3 Analysis of the DinSAR time series

It is noteworthy that all the independent interferograms having significant signals over Kokubu urban area exhibit a phase variation with coherent patterns in both space and time (signal with relatively constant shape and with an amplitude that increases with the time separation between SAR images). In order to better understand and quantify the time de-
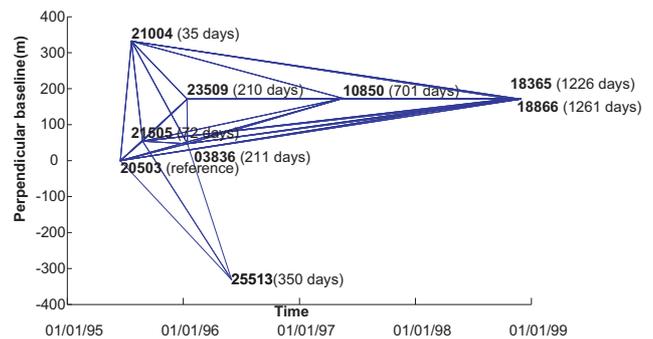

Fig. 3. Dataset of ERS images acquired on the Aira Caldera used in this study (acquisition data versus perpendicular baseline in meters). Solid lines indicate the 31 interferograms used for the time series generation. Time spans in days of each ERS image relative to the reference image orbit 20503 is also reported.

pendency of this interferometry phase signal, we generated a time series relative to the earliest SAR image of our data set (June 1995) using the technique proposed by Lundgren et Usai (2001). First, we selected the most coherent interferograms of our dataset (31 interferograms with perpendicular baseline lower than 400 m, see Fig. 2). The differential interferograms were filtered using a weighted power spectral density filter (Goldstein et al., 1988), and then unwrapped using an implementation of the Network-flow Algorithm for Phase Unwrapping developed by Chen and Zebker (2002). We selected the whole Kokubu urban area where the phase signal is clearly defined. Next, we generated a time series of interferograms relative to the earliest SAR image of our data set (orbit 20503 acquired the 17 June 1995). Due to the
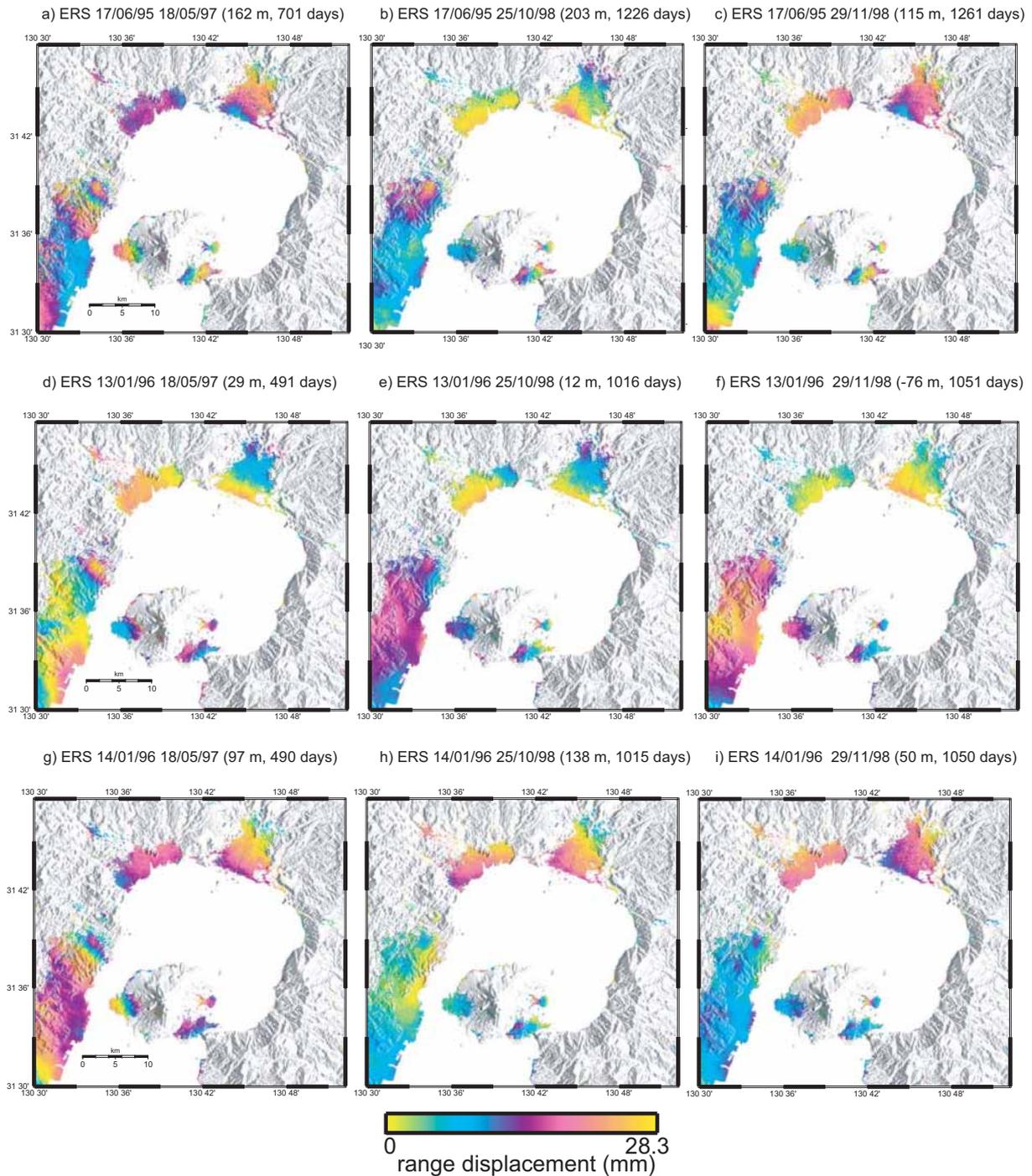
Fig. 4. Recorded differential ERS interferograms over Aira Caldera encompassing the 1995–1998 period: **(a)** interferogram orbits 20503-10850 (period 17 June 1995–18 May 1997, Perpendicular Baseline 162 m, 701 days); **(b)** interferogram orbits 20503–18365 (period 17 June 1995–25 October 1998, Perpendicular Baseline 203 m, 1226 days), **(c)** interferogram orbits 20503–18866 (period 17 June 1995–29 November 1998, Perpendicular Baseline 115 m, 1261 days), **(d)** interferogram orbits 23509–10850 (period 13 January 1996–18 May 1997, Perpendicular Baseline 29 m, 491 days); **(e)** interferogram orbits 23509–18365 (period 13 January 1996–25 October 1998, Perpendicular Baseline 12 m, 1016 days), **(f)** interferogram orbits 23509–18866 (period 23509–29 November 1998, Perpendicular Baseline −76 m, 1051 days), **(g)** interferogram orbits 03836–10850 (period 14 January 1996–18 May 1997, Perpendicular Baseline 97 m, 490 days); **(h)** interferogram orbits 03836–18365 (period 14 January 1996–25 October 1998, Perpendicular Baseline 138 m, 1015 days), **(i)** interferogram orbits 03836–18866 (period 14 January 1996–29 November 1998, Perpendicular Baseline 50 m, 1050 days). A complete cycle of phase (purple, blue yellow) represents a decrease in range of 2.83 cm between the ground surface and the satellite.
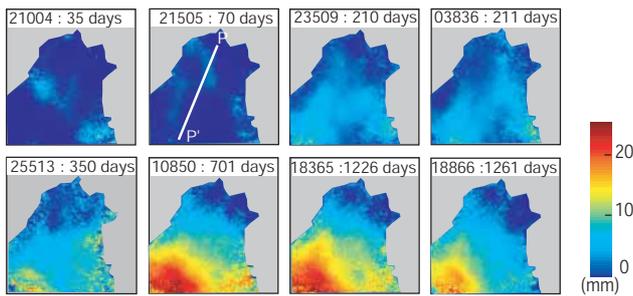
Fig. 5. Inverted displacement field (mm) for each of the 8 ERS images relative to the earliest image (June 1995). Displacements toward the satellite are positive. P and P′ denote the reference profile used in the data analysis.

Fig. 6. Maximum relative ground deformation signal determined from ERS data between north and south Kokubu (PP′ profile) for various acquisition dates. The amplitudes and the standard deviation (vertical error bars) of the maximum uplift values are taken from a 10×50 pixel E-W cross section centered on the area of the maximum uplift around P′. The maximum amplitude of the uplift reaches 23 mm between June 1995 and May 1997.

limited spatial extent of the selected coherent patch it was not possible to define a reference point far away from the area of inflation which could be considered as a zero phase value for the phase unwrapping process. Consequently, in order to make comparable the phase variations both in space and time within the study area and considering the decreasing pattern of the signal towards the north, we defined arbitrarily a reference site on north Kokubu (noted P in Fig. 5) for which the observed deformation is assumed to be minimal over the studied period. The reference phase value for this site has been calculated by averaging the unwrapped phase values for the surrounding pixels within a 200 m squared box. This value has thus been used as a common reference for the whole time series of unwrapped interferograms. By this process, the resulting field displacement maps give a relative measure of the ground displacement with respect to this fixed reference point. In the first stage, in order to detect the presence of noise or unwrapped phase errors that could lead to severe misinterpretations, we estimated the phase unwrapping biases by comparing each subset of three interferograms composed of a linear combination of three SAR images (Lundgren and Usai, 2001). If we have three images (A, B, C) forming interferograms AB, AC, and BC, the absolute deformation at a given pixel for all three interferograms should sum to zero. Since the presence of noise will, in general, result in a non-zero sum, a histogram of the phase sum should show a maximum at the correct phase shift. This analysis enhances the consistency of our dataset of unwrapped interferograms for which a 90% of the pixels have closure discrepancies lower than 4 mm. Next we inverted an InSAR data network, formed by a subset of 31 interferograms. In this way, for a given pixel, the observed displacement is adjusted using a least square inversion to minimize the closure discrepancies within the network. Figure 5 shows the resulting temporal evolution of the displacement field where each image corresponds to the adjusted displacement field relative to the earliest one. The resulting displacement field series clearly reveals a pattern of uplift between June 1995 to November 1999 with as much as 23 mm of dif-
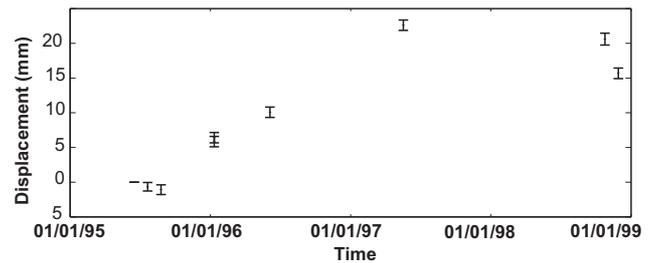
ferential uplift between the south and the north of Kokubu urban area. The Fig. 6 plots the maximum relative ground displacement observed along the P-P′ profile at the respective SAR image acquisition dates. The amplitude and the standard deviation of the differential uplift are taken from a 10×50 pixel cross section centered on the area of the maximum uplift around P′ observed in each adjusted displacement field. The good agreement of measured uplifts obtained for image orbits 23509 and 03836 (8 mm, 6 mm) and images orbits 20503 and 21004 (0 mm, −1 mm) spanning one and 35 days, respectively demonstrates the robustness of the approach. These time series show a differential uplift of up to 23 mm between June 1995 and May 1997 followed by a stop in the uplift observed between May 1997 and October 1998 and finally by a period of an apparent rapid subsidence of few mm amplitude between October and November 1998. Obviously, these estimates must be used with some caution given the uncertainties due to phase delays induced by tropospheric effects. In order to better understand the character of the InSAR data noise in our observations, we examined the spatial structure of interferogram noise in various interferogram which spanned more than one year. We selected sub-images from the southern part of Kagoshima urban area (see Fig. 1). This area was chosen because visual inspection of our series and the results of the previously mentioned studies (Okuyama et al., 2001; Kriswati and Iguchi, 2003) indicate that this area is little affected by deformation. The sub-images have size of 150×150 pixels, or about $7 \text{ km} \times 7 \text{ km}$. Next, we calculated the autocorrelation function of INSAR noise by assuming randomness, following the procedure described in Jonsson (2002). The resulting covariance function estimations show noise variances ranging from 5 to 15 mm^2 and a correlation length scale which varies from 1200 to 1600 m. These results illustrate the variability of the noise structure from one interferogram to another on the study area. Nevertheless, from the result of this analysis, we can estimate the amplitude of the bias induced by noise effects in our
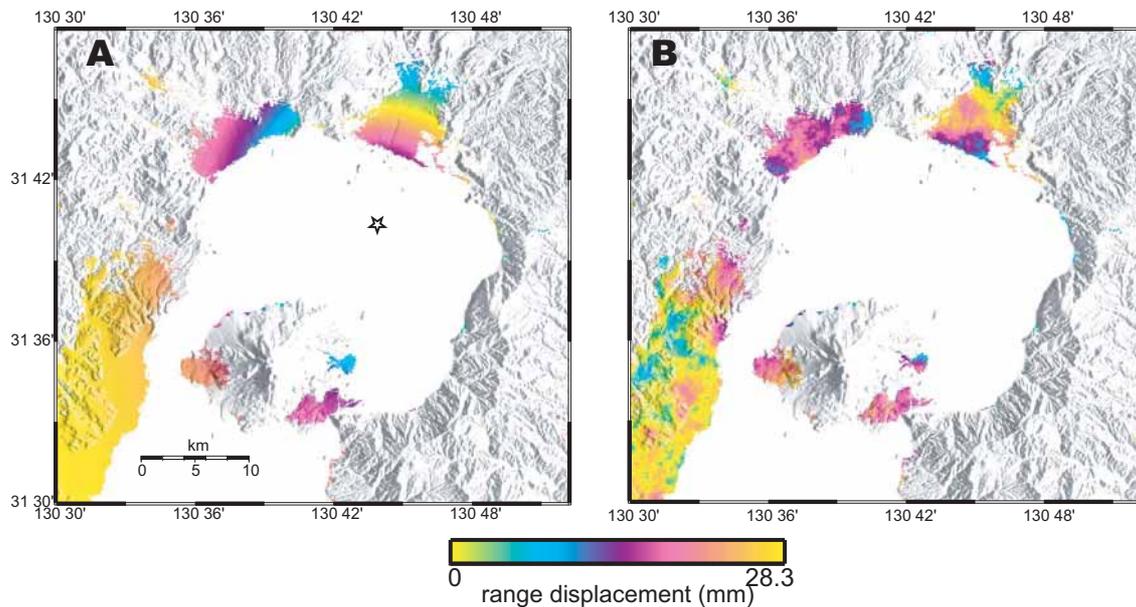
Fig. 7. (a) Simulated interferogram of a Mogi source at 10 km depth with volume change of 25×10^6 m^3. Black star indicates the localisation of the deformation source. (b) A noisy interferogram obtained from addition of (a) and a simulated noise using interferogram noise structure similar to those observed in the study area (variance of 15 mm^2 and correlation length scale of 1600 m). Note that only Kokubu urban area exhibits a phase pattern induced by the volume change within the source. In other areas, the surface deformation signal power is below the detection threshold estimated roughly two or three times the noise variance (30–45 mm^2).
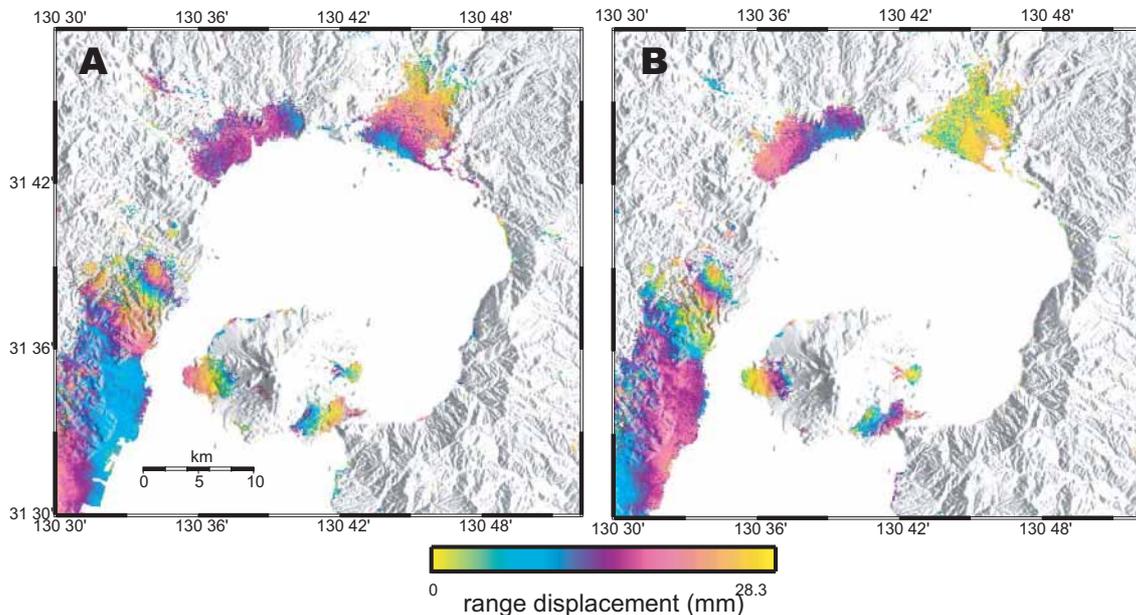

Fig. 8. (a) interferogram orbits 20503–10850. (b) Residual between the best-fit model (volume change of 25×10^6 m$^{3)}$) and the interferogram. The model explains about 68% of the variance in the data. The variance of the residual is about 14 mm^2 consistent with the variance of the interferogram noise derived from our noise analysis. Residual are rewrapped.

estimations of relative displacements between the north and the south of Kokubu to be about 8 mm. This bias and the limited amount of interferograms make the interpretation of the small fluctuation (such as those observed between May 1997 and October 1998 or between October and November 1998) speculative. Nevertheless, considering the magnitude of the decrease in range observed (up to 20 mm) over Kokubu urban area, we interpret the series of temporal signals as mainly

produced by a ground displacement towards the sensor line of sight associated with land uplift. Considering the previous results of other ground deformations studies carried out from JERS and GPS data on this volcanic complex for the similar time period (Okuyama et al., 2001; Kriswati and Iguchi, 2003), we consider that this signal might be consider as a part of a larger ground deformation signal resulting from inflation processes within the main magma chamber below the Aira caldera.

4 Source of crustal deformation

We used a simple approach in order to investigate this hypothesis and to quantify the source for crustal deformations located at the center of the Aira caldera which may produce the observed signal at Kokubu urban area. Such an approach is facilitated by the low topography in the study area that makes possible to use the elastic half space assumption. The limited spatial extent of the coherent area, which will only represent a small segment of the deformation field, makes it impossible to estimate simultaneously the location of the source and its associated variation. We therefore assume then the geometry proposed by Okuyama et al. (2001). Because our observations of the deformation field are discontinuous, it is not obvious how to relate the phase of isolated patches. In order to evaluate the ability of the proposed model and our inversion technique to find a physically acceptable solution, we carried out a synthetic case study. We simulated an interferogram of a Mogi source at 10 km depth for a volume change of 25×10^6 m^3. We added spatially correlated noise with interferogram noise structure similar to those observed previously. Figure 7 shows the small portion of the deformation field measured in the three disconnected patches. Visual inspection reveals that no measurements are available in the two disconnected patches corresponding to Kajiki and Kagoshima urban areas. Clearly the corresponding surface deformation signal power is below the detection threshold, which can be estimated to be roughly two or three times the local noise variance (30–45 mm^2). This explains why the observation of the interferogram series does not reveal a clear deformation pattern over these two disconnected areas. To model the observed deformation, we thus use InSAR phase measurements located in the 10×10 km area used previously, where the signal energy clearly exceeds the noise energy. In the inversion, we use all the interferograms which span more than one year. We solve for the volume change absolute offset of the phase relative to zero deformation. Figure 8 shows the best fit model and the residual for the interferogram formed by images orbits 20503–10850 spanning two years. This model explains 68% of the variance in the data. The variance calculated from the residual (observed – best modeled) data is around 15 mm^2, which is consistent with the variance of the interferogram noise (5 to 15 mm^2) derived from our noise analysis. These values are similar for

Table 1. Inversion solutions for point source models for the subset of the 15 coherent interferograms which span more than one year. Column 2 gives the time spanned by the interferogram in days. Column 3 gives the inferred volume change obtained for each interferogram. Column 4 and 5 give the variance explained by the model and the variance calculated from the residual, respectively. Column 6 gives the inferred rate of volume change.

Master	Slave	days	V ($\times 10^6$ m^3)	Var.exp %	Var.res mm^2	Rate $\times 10^6$ m^3 year^{-1}
20503	10850	701	25	68	14	13
20503	18365	1226	21	60	14	6
20503	18866	1261	19	52	16	5.5
21004	10850	666	30	65	19	16
21004	18365	1191	25	55	19	7.5
21004	18866	1226	18	51	18	5.5
21505	10850	631	27	57	19	15.5
21505	18365	1156	25	63	18	8
21505	18866	1191	19	54	17	6
23509	10850	491	20	84	3	15
23509	18365	1016	18	73	6	6.5
23509	18866	1051	13	64	5	4.5
03836	10850	490	21	79	6	15.5
03836	18365	1015	20	62	12	7
03836	18866	1050	14	48	10	5

most interferograms (see Table 1). We infer the rate of volume change as function of time assuming a constant source depth, a spherical source in half space and a constant rate of deformation during the time period covered in the interferogram. Between 1995 and 1998, there was a roughly constant rate of inflation of about $7–13 \times 10^6$ m^3/year. This estimation is in good agreement with those obtained by other studies based on the analysis of JERS or GPS data spanning similar times:

i) 12×10^6 m^3/year during December 1991–October 1997 (Eto et al., 1998)

ii) $7–16 \times 10^6$ m^3/year between 1992–1998 (Okuyama et al., 2001)

iii) 10×10^6 m^3/year in the January 1998–December 1999 period (Kriswati and Iguchi, 2003)

Figure 9 shows the cumulative volume change of the deformation source during the 1995–2000 period as deduced by the analysis of continuous GPS stations from the permanent Sakurajima monitoring network (Kriswati and Iguchi, 2003). As these series began roughly at the same date than our ERS SAR time series, the results are directly comparable. Our estimations are generally in agreement with those deduced by the analysis of GPS data. For instance, the cumulative volume change of the deformation source during the 1995–1999 period deduced by both analysis is very similar (20×10^6 m^3). Nevertheless, a significant discrepancy is observed in 1997 between both estimations. The value inferred by interferometry is higher than the one inferred by GPS data: 25×10^6 m^3
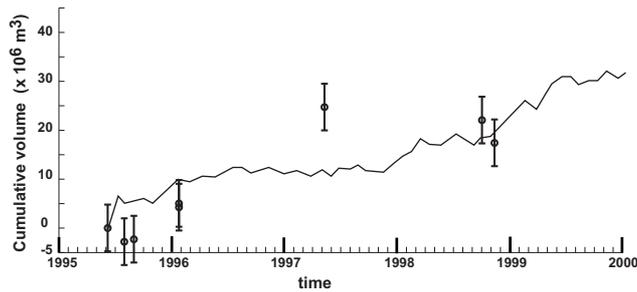
Fig. 9. Thick line shows volume inferred from the analysis of the permanent GPS network (Kriswati and Iguchi, 2003) assuming zero volume at the beginning of the survey (May 1995). Black circles show volume inferred from ERS satellite radar interferometry assuming zero volume at the time of the first SAR images (June 1995). Using the overlapping interferograms, we estimate the rate of deformation between each pair of SAR images with a linear least square inversion. We plot the result as the cumulative volume within the source at the time of each SAR image. We assume a constant error for each measurement of 5×10^6 m^3. As both times series began nearly at the same date, they are directly comparable. Note the agreement between volume inferred from GPS data and those inferred from ERS satellite radar interferometry.

and 11×10^6 m^3; respectively. Due to the limited amount of interferograms in 1997, we can not discard the possibility that an atmospheric signal may be responsible for some of the apparent deformation signal observed over Kokubu urban area in SAR image (orbit 10850) acquired on 18 May 1995.

5 Conclusion

Despite the limited spatial extent of the coherent areas around the Aira Caldera, ERS data has been successfully used in this study for measuring a ground displacement occurring on this volcanic complex during a three year period. The interferogram time series analysis performed on the SAR coherent area of Kokubu city indicates that the south of this city was uplifted by about 20 mm with respect to the northern part. Assuming a spherical model located beneath the center of the Aira Caldera at 10 km depth, we estimate a roughly constant annual rate of inflation of about 5–15×10^6 m^3/year between 1995 and 1998. This estimation is in agreement with those obtained by other studies based on the analysis of JERS or GPS data spanning a similar time period. It is interesting to note that the deformation was observed at least 4 years before the start of the eruption occurred in 1999.

Ground inflation has been commonly observed before the onset of eruption (Lanary et al., 1998; Mann et al., 2002). Nevertheless, further complication the situation numerous studies have shown that some substantial ground deformation can occur due to magma intrusion without eruption (Dvorak and Dzurisin, 1997; Pritchard and Simons, 2002; Langbein,

2003) and others erupt without any deformation being detectable (Pritchard and Simons, 2002). For the Sakurajima volcano, the pattern and rate of surface displacement, which reveal the depth and the rate of pressure increase within the magma reservoir beneath Aira Caldera seems to be a reliable precursor of eruption. In this context, future observations at the Aira Caldera will enable us to learn more details about a typical deformation characteristic of preeruptive inflation and correlation to actual eruptions.

This study clearly shows that data collected in C band by ERS or ENVISAT can give useful constraints on Sakurajima volcano activity and may provide useful additional information to other geodetic measurements to better understand the dynamical processes below the Aira caldera. Although the ERS interferograms exhibit a lower level of coherence than JERS interferograms, the accuracy of the orbital state vectors provided by Delft Institute and the highest sensibility of the C-band to ground deformation enables the detection of subtle crustal deformation signals, such as the one evidenced here

Finally, this study shows that urban areas located around the Sakurjaima volcano may be considered as excellent sites to apply methods more sophisticated than the one used in this study such as those based on InSAR persistent scatterers (Ferretti et al., 2001; Hooper et al., 2004) for analyzing crustal deformation related to Sakurajima volcano activity.

Edited by: T. Van Dam

References

Aramaki, S.: Formation of the Aira Caldera, Southern Kyushu, 22,000 Years ago, J. Geophys. Res., 89(B10), 8485–8501, 1984.

Chen, C. W. and Zebker, H. A.: Phase unwrapping for large SAR interferograms: Statistical segmentation and generalized network models, IEEE Transactions on Geoscience and Remote Sensing, 40, 1709–1719, 2002.

CNES: Philosophie et mode d'emploi de la chaîne logicielle interférométrique DIAPASON (Version 1), Toulouse, France, 1996.

Dvorak, J. J. and Dzurisin, D.: Volcano geodesy: the search for magma reservoirs and the formation of eruptive vents, Rev. Geophys., 35, 343–384, 1997.

Eto, T., Takayama, T., Yamamoto, K., Hendrasto, M., Miki, D., Sonoda, T., Kimata, F., Miyajima, R., Matsushima, T., Uchida, K., Yakiwara, H., and Kokabayasi, K.: On the result of leveling surveys around Sakurajima volcano during December to October 1996, Report of the 9 th joint Observation of Sakurajima Volcano, 1998.

Ferretti, A., Prati, C., and Rocca, F.: Permanent Scattered in SAR interferometry, IEEE Trans. Geosci. Remote Sens, 39(1), 8–20, 2001.

Goldstein, R. M., Zebker, H. A., and Werner, C. L.: Sattelite radar interferometry : two dimensional phase unwrapping, Radio Sci., 23, 713–720, 1988.

Hooper, A., Zebker, H. A., Segall, P., and Kampes, B.: A new method for measuring deformation on volcanoes and other natural terrains using INSAR persitent scatterers, Geophys. Res. Lett., 31(L23611), doi:10.1029/2004GL021737, 2004.

Ishihara, K.: Sakurajima activity for the period from 1995 to 1998, IUGG 22nd General Assembly, Birmingham, UK, 1999.

Jonsson, S.: Modeling volcano and earthquake deformation from satellite radar interferometric observations, PhD thesis, Standford, 174 pp, 2002.

Kriswati, E. and Iguchi, M.: Inflation of the Aira Caldera prior to the 1999 Eruptive Activity at Sakurajima Volcano detected by GPS network in South Kyushu, Disaster Prevention Research Institute Report, 46, 817–825, 2003.

Lanary, R., Lundgren, P., and Sansosti, E.: Dynamic deformation of Etna volcano observed by satellite radar interferometry, Geophys. Res. Lett., 25, 1541–1544, 1998.

Langbein, J. O.: Deformation of the Long Valley Caldera, California: inferences from measurements from 1988 to 2001, Journal of Volcanology and Geothermal Research, 127(3-4), 247–267, 2003.

Lundgren, P. and Usai, S.: Modeling surface deformation observed with synthetic aperture radar interferometry at Campi Flegrei caldera, J. Geophys. Res., 106, 19 355–19 366, 2001.

Mann, C. D., Freymueller, J., and Lu, Z.: Deformation associated with the 1997 eruptio of Okmok volcano, Alaska, J. Geophys. Res., 107(B4), doi:10.1029/2001JB000163, 2002.

Massonnet, D. and Sigmundsson, F.: Remote sensing of volcano deformation by radar interferometry from various satellites, in: Remote Sensing of Active Volcanoes, edited by: Mouginis-Mark, P., Crisp, J. A., and Fink, J. H., Geophys. Monogr., pp. 207–221, 2000.

Matumuto, T.: The four gigantic caldera volcanoes of Kyusyu, Japanese Journal of Geology and Geography, 19, 1–57, 1943.

Mogi, K.: Relations between the eruptions of various volcanoes and the deformation of the ground surface around them, Bulletin Earthquake Research Institute of Tokyo, 36, 99–134, 1958.

Okuyama, S., Takemoto, S., Murakami, M., Tobita, M., Fijuwara, S., Nakagawa, H., and Yarai, H.: Detection of Crustal Deformation in Sakurajima by means of L-band SAR Interferometry based on JERS-1 SAR Images During 1992–1998, INSAR Workshop, Tokyo, Japan, 2001.

Omori, F.: The Sakurajima eruptions and earthquakes, Bull. Volcanol. Soc. Jpn, 8, 1–525, 1916.

Pritchard, M. E. and Simons, M.: A satellite geodetic survey of large scale deformation of volcanic centres in the central Andes, Nature, 418, 167–170, 2002.

Remy, D., Bonvalot, S., Briole, P., and Murakami, M.: Accurate measurement of tropospheric effects in volcanic area from SAR interferometry data: Application to Sakurajima volcano (Japan), Earth Planet. Sci. Lett., 213(3-4), 299–310, 2003.

Schmidt, D. A. and Burgmann, R.: Time-dependant land uplift and subsidence in the Santa Clara valley, California, from a large interferometric synthetic aperture radar data set, J. Geophys. Res., 108, 2416, doi:10.1029/2202JB002267, 2003.

Sharroo, R., Visser, P. N. A. M., and Met, G. J.: Precise orbits determination and gravity field improvement for the ERS satellites, J. Geophys. Res., 103(C), 8113–8127, 1998.

Smithsonian_Institution: Bull. Global Volcanism Network, 24(5), 1999a.

Smithsonian_Institution: Bull. Global Volcanism Network, 24(8), 1999b.

Smithsonian_Institution: Bull. Global Volcanism Network, 25(2), 2000.

Yokoyama, I.: A model for the crustal deformation around volcanoes, J. Phys. Earth, 19, 199–207, 1971.

Zebker, H., Amelung, F., and Jonnson, S.: Remote Sensing of Volcano Surface and Internal Processes Using Radar Interferometry, in: Remote Sensing of Active Volcanoes, edited by: Mouginis-Mark, P., Crisp, J. A., and Fink, J. H., Geophys. Monogr, pp. 179–205, 2000.